Ring Contraction of Metallacyclobutadiene to Metallacyclopropene Driven by π- and σ-Aromaticity Relay

Kaiyue Zhuo
State Key Laboratory of Physical Chemistry of Solid Surfaces, College of Chemistry and Chemical Engineering, Xiamen University, Xiamen, Fujian 361005, China

Yanan Liu
State Key Laboratory of Physical Chemistry of Solid Surfaces, College of Chemistry and Chemical Engineering, Xiamen University, Xiamen, Fujian 361005, China

Kaidong Ruan
State Key Laboratory of Physical Chemistry of Solid Surfaces, College of Chemistry and Chemical Engineering, Xiamen University, Xiamen, Fujian 361005, China

Yuhui Hua
Shenzhen Grubbs Institute, Department of Chemistry, Southern University of Science and Technology, Shenzhen 518055, China

Yu-Mei Lin
State Key Laboratory of Physical Chemistry of Solid Surfaces, College of Chemistry and Chemical Engineering, Xiamen University, Xiamen, Fujian 361005, China

Haiping Xia (hpxia@xmu.edu.cn)
State Key Laboratory of Physical Chemistry of Solid Surfaces, College of Chemistry and Chemical Engineering, Xiamen University, Xiamen, Fujian 361005, China

Article

Keywords:

Posted Date: February 4th, 2022

DOI: https://doi.org/10.21203/rs.3.rs-1276399/v1

Ring Contraction of Metallacyclobutadiene to Metallacyclopropene Driven by π- and σ-Aromaticity Relay

Kaiyue Zhuo,[1,3] Yanan Liu,[1,3] Kaidong Ruan,[1] Yuhui Hua,[2] Yu-Mei Lin,[1]* Haiping Xia[1,2]*

[1]State Key Laboratory of Physical Chemistry of Solid Surfaces, College of Chemistry and Chemical Engineering, Xiamen University, Xiamen, Fujian 361005, China

[2]Shenzhen Grubbs Institute, Department of Chemistry, Southern University of Science and Technology, Shenzhen 518055, China

[3]These authors contributed equally: K. Zhuo, Y. Liu

*Corresponding Authors: linyum@xmu.edu.cn (Y.-M. Lin); hpxia@xmu.edu.cn (H. Xia)

Abstract

π-Aromaticity is an important driving force in directing the synthesis of aromatic compounds; in contrast, reactions induced by σ-aromaticity are uncommon. Herein, we report a strategy based on π- and σ-aromaticity relays to realize the first structurally defined ring contraction of metallacyclobutadiene to metallacyclopropene. This reaction involves the release of the π-antiaromaticity of metallacyclobutadiene in **2a** to afford a π-aromatic intermediate (**4A**), followed by ring reclosure to generate σ-aromatic metallacyclopropene in **3a**. The ring-opening-reclosing mechanism and versatile switching of the aromaticity of the metallacyclic species are supported by

experimental results and theoretical calculations. This work demonstrates the importance of the synergistic effects of π- and σ-aromaticity as driving forces in reactions and sheds light on possible applications in other challenging transformations.

Introduction

Aromaticity is one of the most fundamental and interesting topics in organic chemistry.[1,2] Traditional π-aromaticity is characterized by π-electron delocalization in closed circuits of unsaturated compounds[3] and σ-aromaticity is characterized by the delocalization contributed by σ-electrons, which was first proposed by Dewar to explain the abnormal magnetic behavior of cyclopropane.[4] Subsequently, other systems, such as hydrogen clusters,[5] inorganic rings,[6] metal clusters[7-10] and metallacyclopropenes,[11-14] featuring delocalized σ-conjugation, were suggested to have σ-aromatic character. The terms π- and σ-aromaticity are used to describe the electron delocalization of many cyclic compounds. Both π- and σ-aromaticity endow molecules with aromatic stabilization, leading to products with lower energies. Therefore, aromaticity-driven reactions play a crucial role in synthetic chemistry.[15,16] Currently, π-aromaticity-driven strategies are well known to guide the synthesis of aromatic compounds, but reactions induced by σ-aromaticity have seldom been reported.[17,18]

The synthesis and transformation of small heterocycles are valuable in synthetic chemistry. The small metallacycles, metallacyclobutadienes and metallacyclopropenes are intriguing species because of their rich reactivity and catalytic applications.[19,20] Metallacyclobutadienes are well known in alkyne metathesis[21,22] and polymer

synthesis,[23] while metallacyclopropenes play important roles in organometallic chemistry, such as ring-expansion polymerization for macrocyclic polyenes,[24] selective coupling[25] and activation of C-H bonds.[26] Thus, the synthesis, reactivity, and structural properties of these metallacycles have attracted continuous attention.[27-29] In general, small metallacycles tend to undergo ring expansion by insertion of unsaturated species into the M-C bond or to participate in rearrangement/addition processes, resulting in opening of the metallacycles. On the other hand, the ring-contraction reaction of small metallacycles is challenging due to ring-strain effects, especially in the smallest four-to-three ring-contraction reaction. Considerable effort has been devoted to studying such ring-contraction reactions, such as the migration process in metallacyclobutanes[30] and the conversion of metallacyclobutenes to several metal-allene complexes.[31] However, ring-contraction of metallacyclobutadienes was proposed as a key step only for the formation of metallacyclopropenes via reactions of metal carbynes with alkynes/phosphaalkynes.[32,33] Experimental evidence for the ring contraction of metallacyclobutadienes remains sparse.

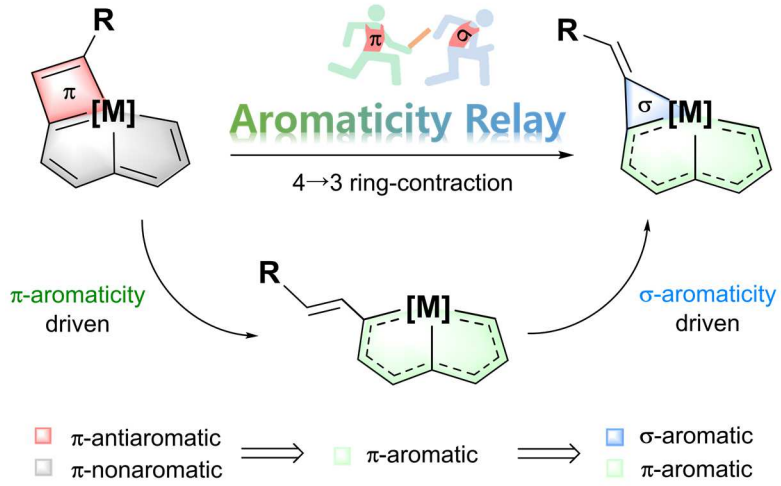

Scheme 1. Aromaticity switching in the ring contraction of metallacyclobutadiene to metallacyclopropene.

Herein, we report a unique π- and σ-aromaticity relay strategy to realize the first structurally defined ring contraction of metallacyclobutadiene to metallacyclopropene (Scheme 1). Combined experimental and computational studies indicate that the transformation occurs via two consecutive steps along a ring-opening-reclosing pathway and involves versatile aromaticity switches in the metallacycles. Initially, the acid-promoted release of the π-antiaromaticity of the osmacyclobutadiene moiety afforded a vinylcarbene fragment. Subsequently, the unusual generation of a strained three-membered ring from vinylcarbene occurred and was found to be driven by the σ-aromaticity of the osmacyclopropene. This synergistic effect of π- and σ-aromaticity driving forces could facilitate the discovery of new reactions, leading to aromatic species that are inaccessible by other methods.

Results and Discussion

Synthesis of precursor 1, [2+2] cycloaddition products 2a–2c and ring-contraction products 3a–3c.

We previously developed a series of aromatic metal bridgehead polycyclic frameworks with a triphenylphosphonium substituent attached to the metallacycle.[34,35] The bulky triphenylphosphonium group stabilizes the metallacyclic skeletons but may reduce the reactivity due to its steric and electron-withdrawing properties. Accordingly, we designed and synthesized an osmapentalyne (**1**) with a chlorine substituent instead of triphenylphosphonium at C2 through the treatment of $OsCl_2(PPh_3)_3$ with a multiyne (**L1**) in the presence of excess tetrabutylammonium chloride. The structure of **1** was

identified by nuclear magnetic resonance (NMR) spectroscopy and high-resolution mass spectrometry (HRMS). When osmapentalyne **1** was treated with different terminal alkynes, including *p*-toluenesulfonylacetylene, methyl propiolate and propiolic acid, all bearing electron-deficient groups, the [2+2] cycloaddition reactions occurred within 5 min, affording osmacyclobutadienes **2a**–**2c** in high yields (>90%) (Figure 1a).

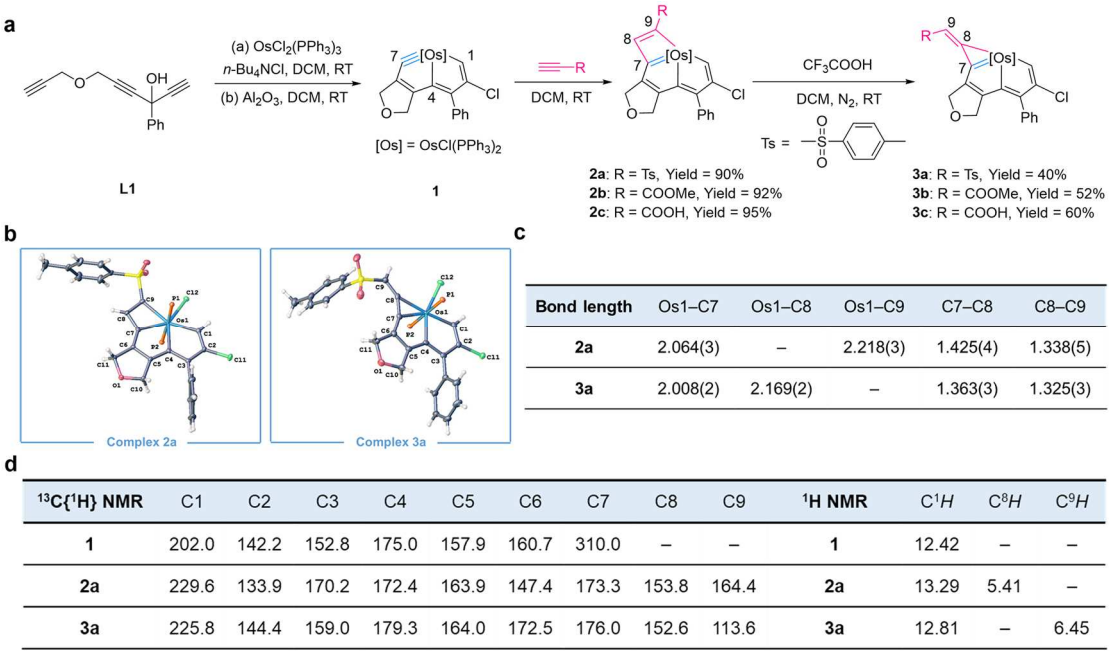

Bond length	Os1–C7	Os1–C8	Os1–C9	C7–C8	C8–C9
2a	2.064(3)	–	2.218(3)	1.425(4)	1.338(5)
3a	2.008(2)	2.169(2)	–	1.363(3)	1.325(3)

$^{13}C\{^1H\}$ NMR	C1	C2	C3	C4	C5	C6	C7	C8	C9	^1H NMR	C^1H	C^8H	C^9H
1	202.0	142.2	152.8	175.0	157.9	160.7	310.0	–	–	**1**	12.42	–	–
2a	229.6	133.9	170.2	172.4	163.9	147.4	173.3	153.8	164.4	**2a**	13.29	5.41	–
3a	225.8	144.4	159.0	179.3	164.0	172.5	176.0	152.6	113.6	**3a**	12.81	–	6.45

Fig. 1 | Synthesis and characterization of 1, 2a–2c and 3a–3c. a, Synthesis of osmapentalyne **1** and its reactions with alkynes *via* formal [2+2] cycloaddition to yield complexes **2a**-**2c** and the synthesis of **3a**-**3c** by reactions of **2a**-**2c** with CF_3COOH. **b**, X-ray crystal structures for **2a** and **3a** drawn at the 50% probability level. The phenyl groups in PPh_3 have been omitted for clarity. **c**, Selected bond lengths (Å) for **2a** and **3a**. **d**, Selected NMR chemical shifts (ppm) for **1**, **2a** and **3a**.

The structure of complex **2a** was confirmed by single-crystal X-ray diffraction analysis. As shown in Figure 1b, complex **2a** has a planar metallatricyclic structure, as reflected by the mean deviation from the least-squares plane (0.022 Å) through Os1 and C1–C9. In the four-membered ring (4MR) of **2a**, the bond lengths of Os1–C7 (2.064 Å), Os1–C9 (2.218 Å), C7–C8 (1.425 Å) and C8–C9 (1.338 Å) are all comparable to those reported for osmacyclobutadienes (Figure 1c).[36] The structure of complex **2a** was

99 further supported by NMR spectroscopy. In the ^{1}H NMR spectrum, the singlet signal
100 attributed to C^{1}*H* at δ = 13.29 ppm was assigned to Os*CH*.[36] In the ^{13}C{^{1}H} NMR
101 spectrum, the characteristic signal of C7 in **2a** was observed at δ = 173.3 ppm, shifting
102 136.7 ppm to a higher field compared to the signal of C7 in complex **1** (310.0 ppm),
103 revealing the conversion from metal carbyne to metal carbene. The main NMR
104 chemical shifts (δ) of **1** and **2a** are shown in Figure 1d. The [2+2] cycloaddition reaction
105 of metal carbynes with alkynes has been used to synthesize metallacyclobutadienes
106 containing, for example, Ta, Mo, W and Re.[19] In contrast, this method has rarely been
107 used for the synthesis of metallacyclobutadienes containing late transition metals,[36-38]
108 whose reactivity has rarely been studied. With osmacyclobutadienes **2a**–**2c** in hand, we
109 investigated their chemical reactions.

110 Complexes **2a**–**2c** were treated with 10 equiv. of CF_3COOH in CH_2Cl_2 at rt for 3
111 h, resulting in reddish-brown complexes **3a**–**3c** in isolated yields of 40-60% (Figure 1a).
112 The structure of **3a** was confirmed by single-crystal X-ray diffraction. As shown in
113 Figure 1b, the metal was shared by the propene and pentalene rings in **3a**. Similar to
114 that in **2a**, ring contraction involves the cleavage of Os1–C9 and the formation of Os1–
115 C8. The ten atoms (Os1 and C1–C9) in **3a** are almost coplanar, and the mean deviation
116 from the least-squares plane is only 0.025 Å. The Os1–C7 distance (2.008 Å) of **3a** is
117 shorter than the Os1–C7 distance (2.064 Å) of **2a**, indicating some Os=C double bond
118 character.[39] Compared to the Os1–C9 distance (2.218 Å) of **2a**, the Os1–C8 distance
119 (2.169 Å) of **3a** is shorter and is characteristic of metallacyclopropenes (Figure 1c). The
120 C7–C8 bond length of 1.363 Å is similar to that of previously reported fused

osmacyclopropenes.[11-14,40] The C8–C9 bond length (1.325 Å) is typical of C=C double bonds. The ^{1}H NMR spectrum of **3a** displays a characteristic signal at δ = 12.81 ppm attributed to C^{1}*H*. Both the C^{9}*H* and C9 signals at δ = 6.45 and 113.6 ppm, respectively, suggest that C9 is a vinyl carbon atom. Similar structures of **3b** and **3c** were also determined by single-crystal X-ray diffraction (Supplementary Figs. S3 and S4).

Chemical reactions of metallacyclobutadienes have been investigated previously, including the dissociation of alkynes to afford carbyne complexes,[21,22] alkyne/CO insertion and the formation of metallabenzenes/other cyclic carbene complexes or reductive elimination products, such as η^{5}-cyclopentadienyl and η^{3}-cyclopropenyl complexes.[41,42] Metallacyclobutadienes have also been proposed as intermediates in the formation of vinylcarbene complexes[43] or metallacyclopropenes from reactions of metal carbynes with alkynes/phosphoalkynes.[32,33] In principle, metallacyclobutadienes tend to undergo ring expansion or ring opening. In fact, to the best of our knowledge, the transformation of **2a** to **3a** represents the first observation of a structurally well-defined ring contraction of metallacyclobutadiene to metallacyclopropene. In addition, metallacyclopropenes have usually been synthesized by the direct [2+1] addition of an alkyne to a metal center.[28,29] The formation of **3a**–**3c** by an unprecedented ring contraction process provides a new strategy to synthesize metallacyclopropenes.

Verification of the mechanism by theoretical calculations and the isolation of key intermediates.

DFT calculations were performed to investigate the mechanism of the formation of **3a**.

The computed Gibbs free energy profile of the key reaction steps is shown as a black line in Figure 2a. The initial attack of CF_3COOH led to the cleavage of the Os–C9 single bond in **2a** and the formation of C9-H, generating **Int 4a** *via* a transition state (**TS1**). The protonation process has an energy barrier of 14.2 kcal mol^{-1} and is exergonic by 9.9 kcal mol^{-1}; therefore, this reaction is theoretically facile. Subsequently, elimination of C^8H yields the final energetically favorable product (**3a**) from **Int 4a** with an energy barrier of 10.7 kcal mol^{-1}, and this process is exergonic by 16.9 kcal mol^{-1}.

Control experiments were performed to further confirm the proposed mechanism. Different amounts of acids were tested in reactions monitored by $^{31}P\{^1H\}$ NMR spectroscopy. As shown in Figure 2c, upon reaction of complex **2a** with 10 equiv. of CF_3COOH, product **3a** was obtained exclusively. However, when the reaction was carried out in the presence of 20 equiv. of CF_3COOH, a new singlet at 17.45 ppm in the $^{31}P\{^1H\}$ NMR spectrum, attributed to species **4a**, was observed. A series of parallel experiments showed that the content of **4a** increased gradually as the amount of acid increased. When the acid level exceeded 50 equiv., the relative ratio of **3a** and **4a** remained almost unchanged. It can be assumed that the excess acid stabilized intermediate **4a**. When dilution experiments were conducted by the addition of CH_2Cl_2 to the reaction mixture of **3a** and **4a**, compound **4a** was gradually converted into **3a** with decreasing acid concentration. Based on these results, **4a** was concluded to be an intermediate in the formation of **3a**, and the transformation from intermediate **4a** to final product **3a** was inhibited by excess CF_3COOH. Other acids were tested in the formation of **4a**. Fortunately, upon treatment of **2a** with excess $HBF_4{\cdot}Et_2O$, a **4a** analog

named **4A** was isolated as the main product. This analog was completely converted into **3a** by heating the *in situ* mixture to 40 °C (Figure 2b).

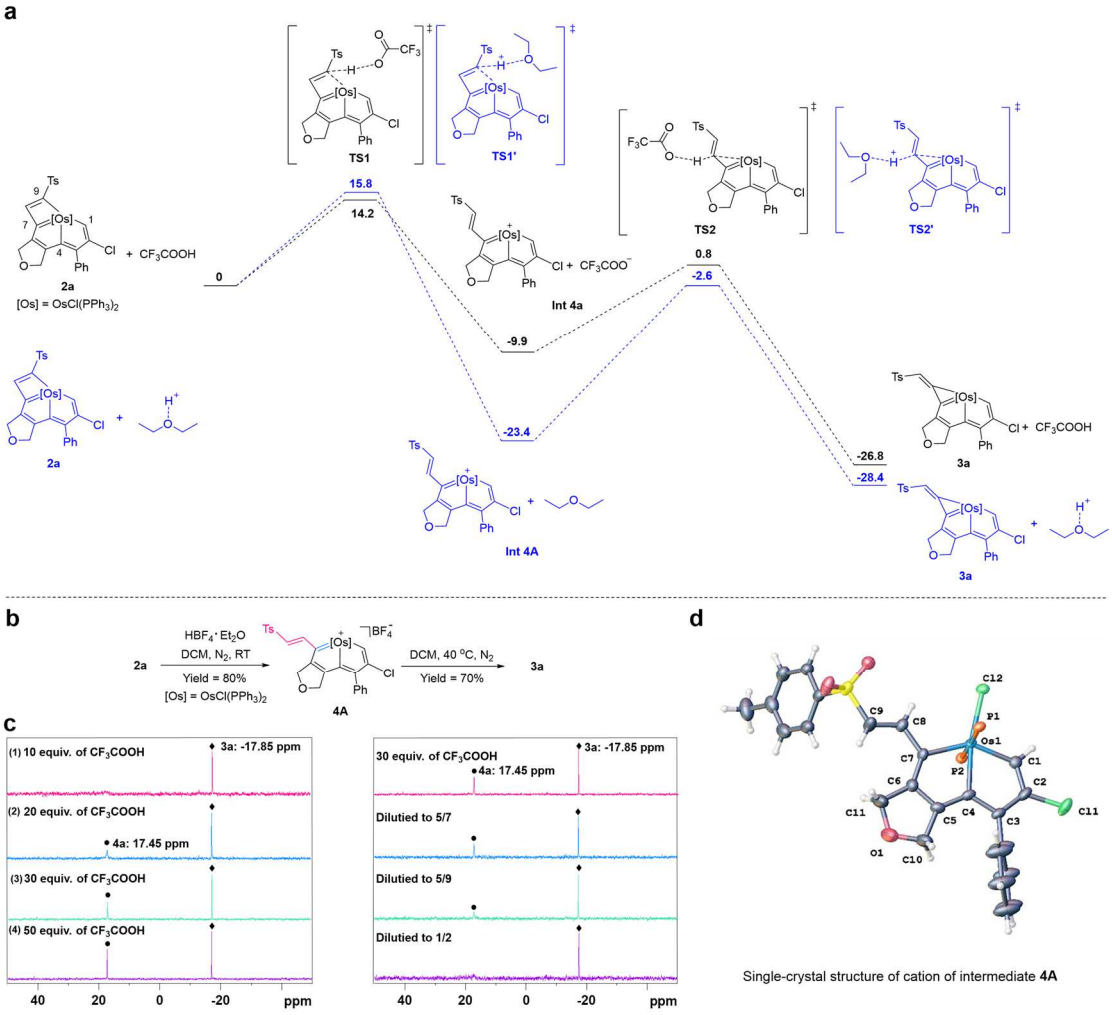

Fig. 2 | Mechanistic investigation: DFT calculations, control experiments and the isolation of key intermediates 4A. a, Energy profiles for the formation of complex **3a** in the presence of CF_3COOH (black) or $HBF_4{\cdot}Et_2O$ (blue). Energies are given in kcal mol^{-1}. The Gibbs free energy of reactant **2a** with acid (CF_3COOH or $HBF_4{\cdot}Et_2O$) was designated as 0 kcal mol^{-1}. The B3LYP-D3/Def2-TZVP method with SMD solvation in CH_2Cl_2 was used. **b**, ring-contraction of **2a**–**2c** to **3a**–**3c** through a stepwise pathway involving the ring-opening product of **4A** induced by $HBF_4{\cdot}Et_2O$. **c**, investigation of the formation of **4a** by $^{31}P\{^1H\}$ NMR spectroscopy. Parallel reactions of 10, 20, 30 and 50 equiv. of CF_3COOH with **2a** (left). The *in situ* reaction system (30 equiv. of CF_3COOH with **2a**) was diluted to 5/7, 5/9 and 1/2 of its original concentration (right). **d**, X-ray crystal structure of cation of intermediate **4A** drawn at the 50% probability level. The phenyl groups in PPh_3 have been omitted for clarity.

Single-crystal X-ray diffraction showed that **4A** is an osmapentalene bearing a vinyl group attached at C7. As shown in Figure 2d, the metal is coordinated with six atoms, namely, three carbon atoms (C1, C4 and C7), two phosphorus atoms and a

chlorine atom, leading to a coordinated unsaturated 16 electron osmium center. The bond lengths of Os1–C1 (1.962 Å) and Os1–C7 (2.021 Å) are comparable to previous observations in osmapentalenes (1.926–2.084 Å).[44] The C8–C9 bond length (1.323 Å) is consistent with that of a typical C=C double bond. The C7–C8 bond connects the metallabicycle with a vinyl group, and the distance (1.464 Å) indicates a C–C single bond. In the ^{1}H NMR spectrum, the two doublets at δ = 6.99 and 6.10 ppm were assigned to C8*H* and C9*H,* respectively. The coupling constant of *H*C8=C9*H* group was 14.40 Hz, confirming the E-isomer configuration. All the data confirm that the cation of structure **4A** is identical to that of **Int 4a** in the proposed mechanism.

Additional DFT calculations were performed to examine the formation of **3a** under acidic conditions in the presence of $HBF_4 \cdot Et_2O$ (blue line in Figure 2a). The formation of **3a** through **TS1'** was associated with a much higher exothermicity of 23.4 kcal mol^{-1} to form **Int 4A** than to form **Int 4a** (9.9 kcal mol^{-1}). The species **Int 4A** is thermodynamically favored and is more stable than **Int 4a**. In addition, the conversion of **Int 4A** to **3a** *via* **TS2'** proceeded with a significantly higher computed barrier of 20.8 kcal mol^{-1} (10.7 kcal mol^{-1} for **TS2**); thus, **Int 4A** can be readily isolated and characterized, and it's consistent with our experimental studies showing that producing **3a** required heating (Figure 2b).

The combined experiments and DFT calculations confirmed that ring contraction proceeds through a ring-opening-reclosing pathway involving acid-mediated protonation and deprotonation *via* vinylcarbene species (**4A**). Notably, the Gibbs free energy profile suggested that **3a**, with a strained metallacyclopropene, is more stable

than **4A**. To address this issue, the aromaticity of each of these species was investigated.

Theoretical studies of aromaticity.

Nucleus-independent chemical shift (NICS) calculations[45] were performed based on simplified model compounds **2a'**, **3a'** and **4A'**, in which PH_3 groups were used to replace the PPh_3 ligands and the phenyl ring attached to C3 was omitted. In general, negative NICS values indicate aromaticity, while positive NICS values represent antiaromaticity. As shown in Figure 3a, the positive $NICS(1)_{zz}$ value of the fused 4MR (+25.8 ppm) suggests antiaromaticity in the fused metallacyclobutadiene in complex **2a'**. The $NICS(1)_{zz}$ values of the two fused five-membered rings (5MR) (-3.7 and 3.3 ppm) imply nonaromaticity. In sharp contrast, the two fused 5MRs of **4A'** show $NICS(1)_{zz}$ to have significantly reduced negative values (-15.1 and -22.6 ppm), revealing the aromaticity of **4A'**. The ring-opening of the 4MR relieves the antiaromaticity of the metallacyclobutadiene in **2a'** and results in enhancement of the aromaticity of the two 5MRs in **4A'**. The new generation of the aromatic 3MR in **3a'** is supported by the negative $NICS(1)_{zz}$ value of -30.4 ppm. The other two fused 5MRs of **3a'** with large negative $NICS(1)_{zz}$ values of -17.0 and -17.6 ppm suggest that the aromaticity is maintained. Coincidentally, the $NICS(1)_{zz}$ grids demonstrate that the inner cavity area of metallacyclobutadiene in **2a'** is deshielded (red, positive values), while the inner cavity area of metallacyclopropene in **3a'** is shielded (blue, negative values) (Figure 3a). Anisotropy of the induced current density (AICD)[46] analysis also supported the aromaticity changes in these complexes (Figure 3b). Distinct

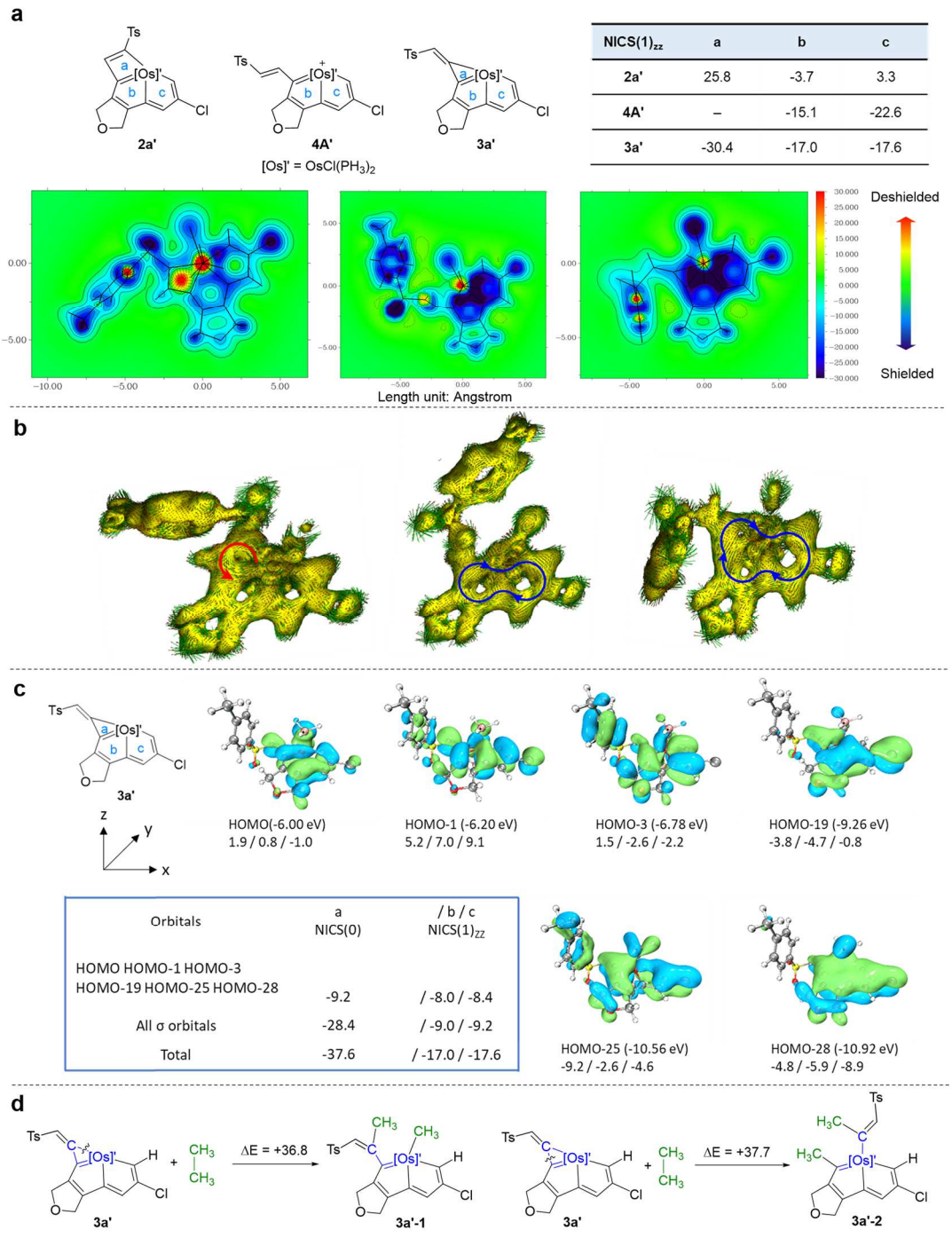

Fig. 3 | Aromaticity evaluation. a, NICS(1)$_{zz}$ values and NICS(1)$_{zz}$ grids for model compounds **2a'**, **4A'** and **3a'** (NICS(1)$_{zz}$ calculated at 1.0 Å above the ring centers. Each grid is parallel to the fused ring with 0.01 Å resolution and 40000 points. A fixed color scale (−30.000 to +30.000 ppm) is used in all grids for a visualized comparison. Projections of the framework are presented on the maps and connected by lines). **b**, The AICD plots of **2a'**, **4A'** and **3a'**. The isosurface value of the AICD plots is 0.030 a.u. The magnetic field vector is orthogonal with respect to the ring plane and is directed upward (the corresponding paratropic (red arrow) and diatropic (blue arrow) ring currents are shown). **c**, key occupied π MOs and their energies together with their contributions to NICS(0) and NICS(1)$_{zz}$ (in ppm) for model complex **3a'**. The eigenvalues of the MOs are given in parentheses in the first line, and the NICS(0) and NICS(1)$_{zz}$ values of rings a, b, and c are given in the second line. **d**, Isodesmic reactions for **3a'** (all energies are given in kcal mol^{-1}).

counterclockwise circulation of **2a'** was observed in the fused osmacyclobutadiene, suggesting antiaromaticity, whereas the clockwise circulation observed in two fused 5MRs demonstrated the aromaticity of **4A'**, and the clockwise circulation along the periphery of the whole metallatricycle of **3a'** indicated expansion of the global aromaticity.

To further examine our hypothesis of the aromaticity of complex **3a'**, canonical molecular orbital (CMO) NICS calculations were performed to identify the σ and π orbital contributions separately (Figure 3c). The dissected NICS(0) and $NICS(1)_{zz}$ were selected to evaluate the nature of the possible σ-aromaticity in the 3MR. The total diamagnetic contribution of the NICS(0) value for the 3MR from the six occupied π molecular orbitals (HOMO, HOMO-1, HOMO-3, HOMO-19, HOMO-25, and HOMO-28) was -9.2 ppm, whereas the NICS(0) value from all the σ-orbitals (-28.4 ppm) was much more negative, indicating that σ-aromaticity is dominant in the 3MR and is the major contribution to aromaticity in the 3MR in **3a'**. The results are consistent with the σ-aromatic character of reported metallacyclopropenes.[11-14] The stability of osmacyclopropene in **3a'** can be investigated by means of two isodesmic reactions (Figure 3d). The endothermic (+36.8 and +37.7 kcal mol^{-1}) nature of the cleavage of the Os–C or C–C bonds in the 3MR in these isodesmic reactions also confirms the aromatic stabilization of the osmacyclopropene unit.[47]

Theoretical calculations indicated that aromaticity plays an important role in lowering the energy associated with the transformation of **2a** → **3a**. The ring-opening of osmacyclobutadiene in **2a** to form **4A** involves the release of antiaromaticity

accompanied by the reinforcement of the π-aromaticity in osmapentalene and can be viewed as a π-aromaticity-driven process. Next, the ring-reclosing process from **4A** → **3a** further expands the aromaticity system of the metallacycles with newly formed σ-aromaticity. Thus, the ring-contraction reaction is driven by the relay of π- and σ-aromaticity, which is readily achieved because it lowers the potential energies smoothly with no high barriers.

Thermal and chemical stability and optical properties.

Thermal stability tests indicated that aromatic species **3a**–**3c** are significantly more stable than complexes **2a**–**2c**. In the solid state, complexes **2a**–**2c** are stable at rt and start to decompose at 100 °C for **2a** and **2c** or 110 °C in the case of **2b**. In comparison, complexes **3a**–**3c** exhibit higher thermal stability even when heated to 180 °C in the case of **3a**, 160 °C for **3b** and 140 °C for **3c** in air for 3 h (Supplementary Fig. S11).

In addition, the chemical reactivity of **3a** was investigated. Treatment of **3a** with *N*-chlorosuccinimide (NCS) or *N*-bromosuccinimide (NBS) led to the formation of complexes **5a** and **5b**, respectively, in high yields (both are 95%) (Figure 4a). The structure of **5b** shows that C9 is now substituted by a bromine atom, indicating the electrophilic substitution of the vinyl group. Treatment of **3a** with excess 2,3-dichloro-5,6-dicyano-1,4-benzoquinone (DDQ) at 40 °C led to the formation of complex **6a**. As shown in Figure 4b, the bond lengths of C10–O1 and C11–O2 (1.162 and 1.193 Å, respectively) indicated the C=O double bond character, confirming that the 2,5-dihydrofuran unit of complex **3a** was oxidized to form aldehydes. The NMR spectrum

showed peaks attributed to C10*H* and C11*H* at δ = 9.04 and 10.00 ppm, respectively, and together with the signals of C10 (δ = 192.7 ppm) and C11 (188.9 ppm), they can be attributed to the two aldehyde groups. Electrophilic substitution and an oxidation reaction both occurred at the exocyclic positions of **3a**, suggesting the high stability and resistance to oxidation of the metallatricyclic moiety, in accordance with its aromatic character.

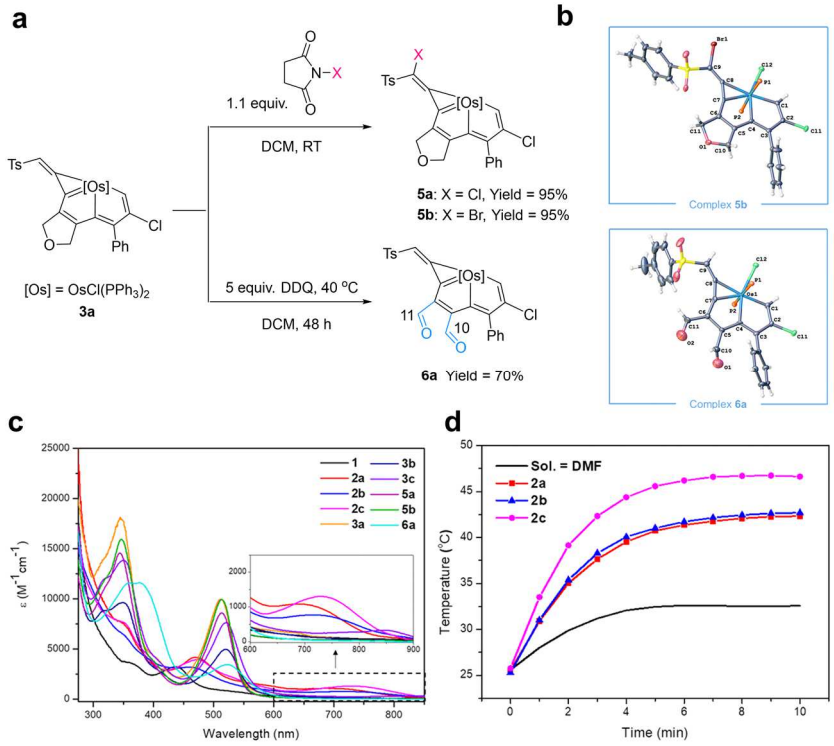

Fig. 4 | Chemical stability and optical properties. a, Electrophilic substitution and oxidation reaction of **3a**. **b**, X-ray crystal structure of complexes **5b** (top) and **6a** (down) drawn with 50% probability level. The phenyl groups in PPh_3 have been omitted for clarity. **c**, UV–Vis absorption spectra for **1**, **2a**–**2c** (2.0×10^{-4} M) and **3a**–**3c**, **5a**, **5b**, **6a** (4.5×10^{-5} M) measured in CH_2Cl_2 at rt. **d**, Temperature curves for **2a**–**2c** (1.00 mg mL^{-1}) irradiated by an 808 nm laser at a power density of 1.0 W cm^{-2} in DMF.

The UV–Vis absorption spectra of metallacycles **2a**–**2c** display an absorption maximum λ_{max} at approximately 470 nm, slightly redshifted compared with that of osmapentalyne (**1**) (Figure 4c). They also have weak and broad absorption band tails at 700–800 nm, which are typical bathochromic shifts of NIR bands attributed to the

decrease in optical band gaps, in accordance with the antiaromatic character.[48,49] The NIR absorption of **2a**–**2c** exhibits photothermal properties; for example, the temperature of the solution containing 1.00 mg mL^{-1} for **2c** increased from 25.5 °C to 46.6 °C within 7 min under irradiation at 808 nm by a laser at a laser power density of 1.0 W cm^{-2} (Figure 4d). Metallacycles **3a**–**3c** gave rise to two obvious absorption peaks at wavelengths of ~340 and ~510 nm. Compared with **3a**, electrophilic substitution products **5a** and **5b** exhibited similar absorption properties, while the oxidation product **6a** gave rise to two slightly redshifted broad absorption peaks.

Conclusion

In summary, we have described an unusual acid-induced ring contraction of metallacyclobutadiene to metallacyclopropene *via* a ring-opening-reclosing process. The successful isolation of the key intermediate and the results of theoretical calculations confirm that the driving force of aromatization plays a vital role in the reaction. The π-aromaticity-driven ring opening of an antiaromatic metallacyclobutadiene followed by σ-aromaticity-driven ring-reclosing resulted in the expansion of global aromaticity. Versatile aromaticity switches in these metallacycles have been observed, i.e., from π-anti-/nonaromaticity to π-aromaticity and further π- and σ-aromaticity. These findings offer a valuable supplement to the ring contraction in small metallacycles and provide new insight into aromaticity-driven relay strategies and their potential application in challenging transformations.

Methods

General methods. Compounds **S-1**, **S-2** and **L1** were synthesized according to the literature.[15] Details of the synthesis and characterization of compounds in this article as **S-1**, **S-2**, **L1, 2a**–**2c**, **3a**–**3c**, **4A**, **5a**, **5b** and **6a** can be found in the Supplementary Information (SI). For general information, synthesis and characterization, see pages S2-S11. For control experiments, see Figs. S1-S3. For crystallographic analysis, see Figs. S4-S10 and Tables S1-S10. For thermal stability tests, see Figs. S11. For computational methods, see Figs. S12-S14. For NMR spectra and ESI-MS spectra, see Figs. S15-S61. The X-ray crystal structures have been deposited in the Cambridge Crystallographic Data Centre (CCDC) and identified as 2103042 (**2a**), 2103166 (**3a**), 2103167 (**3b**), 2103168 (**3c**), 2103171 (**4A**), 2103169 (**5b**) and 2103170 (**6a**). These data can be obtained free of charge from the Cambridge Crystallographic Data Centre via www.ccdc.cam.ac.uk/data_request/cif.

Synthesis of complex 1. Under a N_2 atmosphere, a mixture of **L1** (256 mg, 1.14 mmol), $OsCl_2(PPh_3)_3$ (1.00 g, 0.95 mmol) and *n*-Bu_4NCl (1.00 g, 3.60 mmol) was stirred in CH_2Cl_2 (25 mL) at rt for 15 min to give a brown solution. The solution was evaporated under vacuum to a volume of approximately 2 mL. Then, the solution was purified by column chromatography (alumina gel, eluent: CH_2Cl_2) to give **1** (425 mg, 45%) to obtain a yellow solid.

Synthesis of complex 2a: Under a N_2 atmosphere, a mixture of complex **1** (500 mg, 0.50 mmol) and *p*-toluenesulfonylacetylene (400 mg, 2.50 mmol) was stirred in CH_2Cl_2 (25 mL) at rt for 5 min to give a brown solution. The solution was evaporated under

vacuum to a volume of approximately 2 mL. Then a mixed solvent (Et_2O/PE = 1:4, v/v, 50 mL) was added to the solution. The brown precipitate was collected by filtration, washed with mixed solvent (Et_2O/PE = 1:4, v/v, 2 × 50 mL) and dried under vacuum to give **2a** (527 mg, 90%) as a brown solid.

Synthesis of complex 3a. Under a N_2 atmosphere, trifluoroacetic acid (500 μL, 6.73 mmol) was added to a solution of complex **2a** (500 mg, 0.43 mmol) in CH_2Cl_2 (25 mL). The reaction mixture was stirred at rt for 3 h to give a mandarin red solution. The solution was evaporated under vacuum to a volume of approximately 2 mL. Then the solution was purified by column chromatography (silica gel, eluent: CH_2Cl_2 and CH_2Cl_2/Me_2CO = 100:1, v/v) to give **3a** (200 mg, 40%) as a reddish-brown solid.

Synthesis of complex 4A. Under a N_2 atmosphere, a solution of $HBF_4 \cdot Et_2O$ (50-55% w/w HBF_4, 100 μL, 0.60 mmol) was added to a solution of complex **2a** (50 mg, 42.5 μmol) in CH_2Cl_2 (0.5 mL). The reaction mixture was stirred at rt for 30 min to give an orange solution of **4A** (approximately 80% yield based on ^{1}H- and ^{31}P-NMR), which was characterized by *in situ* ^{1}H-NMR, ^{31}P-NMR and ^{13}C-NMR. Complex **4A** is stable only under strong acidic conditions.

Data Availability

The data supporting the findings of this study are available from the corresponding author upon request.

References

1. Schleyer, P. v. R. Introduction: Aromaticity. *Chem. Rev.* **101**, 1115-1118 (2001).

2. Pagano, J. K. *et al*. Actinide 2-metallabiphenylenes that satisfy Hückel's rule. *Nature* **578**, 563-567 (2020).

3. Hückel, E. Quantentheoretische Beiträge zum Benzolproblem. *Z. Phys. A: Hadrons Nucl.* **70**, 204-286 (1931).

4. Dewar, M. J. S. Chemical Implications of σ Conjugation. *J. Am. Chem. Soc.* **106**, 669-682 (1984).

5. Havenith, R. W. A., De Proft, F., Fowler, P. W. & Geerlings, P. σ-Aromaticity in H_3^+ and Li_3^+: Insights from ring-current maps. *Chem. Phys. Lett.* **407**, 391-396 (2005).

6. Li, Z. H., Moran, D., Fan, K. N. & Schleyer, P. v. R. σ-Aromaticity and σ-Antiaromaticity in Saturated Inorganic Rings. *J. Phys. Chem. A*. **109**, 3711-3716 (2005).

7. Boldyrev, A. I. & Wang, L. S. All-Metal Aromaticity and Antiaromaticity. *Chem. Rev.* **105**, 3716-3757 (2005).

8. Boronski, J. T., Seed, J.A., Hunger, D. *et al*. A crystalline tri-thorium cluster with σ-aromatic metal–metal bonding. *Nature* **598**, 72–75 (2021).

9. Freitag, K. *et al*. The σ-Aromatic Clusters $[Zn_3]^+$ and $[Zn_2Cu]$: Embryonic Brass. *Angew. Chem., Int. Ed.* **54**, 4370-4374 (2015).

10. Popov, I. A. *et al*. Peculiar All-Metal σ-Aromaticity of the $[Au_2Sb_{16}]^{4-}$ Anion in the Solid State. *Angew. Chem., Int. Ed.* **55**, 15344-15346 (2016).

11. Zhu, C. *et al*. σ-Aromaticity in an Unsaturated Ring: Osmapentalene Derivatives

376 Containing a Metallacyclopropene Unit. *Angew. Chem., Int. Ed.* **54**, 3102-3106
377 (2015).
378 12. Hao, Y., Wu, J. & Zhu, J. σ Aromaticity Dominates in the Unsaturated Three-
379 Membered Ring of Cyclopropametallapentalenes from Groups 7-9: A DFT Study.
380 *Chem. - Eur. J.* **21**, 18805-18810 (2015).
381 13. Chu, Z., He, G., Cheng, X., Deng, Z. & Chen, J. Synthesis and Characterization of
382 Cyclopropaosmanaphthalenes Containing a Fused σ-Aromatic Metallacyclopropene
383 Unit. *Angew. Chem., Int. Ed.* **58**, 9174-9178 (2019).
384 14. Bao, X. *et al.* One-pot syntheses of rhena-2-benzopyrylium complexes with a fused
385 metallacyclopropene unit. *Chem. Commun.* **57**, 1643-1646 (2021).
386 15. Zhuo, Q. *et al*. Multiyne chains chelating osmium via three metal-carbon σ bonds.
387 *Nat. Commun.* **8**, 1912 (2017).
388 16. Hein, S. J., Lehnherr, D., Arslan, H., F, J. U.-R. & Dichtel, W. R. Alkyne
389 Benzannulation Reactions for the Synthesis of Novel Aromatic Architectures. *Acc.*
390 *Chem. Res.* **50**, 2776-2788 (2017).
391 17. Xu, H. L. *et al*. σ-Aromaticity-Induced Stabilization of Heterometallic
392 Supertetrahedral Clusters $[Zn_6Ge_{16}]^{4-}$ and $[Cd_6Ge_{16}]^{4-}$. *Angew. Chem., Int. Ed.* **59**,
393 17286-17290 (2020).
394 18. Jian, T. *et al*. $Nb_2@Au_6$: a molecular wheel with a short Nb≡Nb triple bond
395 coordinated by an Au_6 ring and reinforced by σ Aromaticity. *Chem. Sci.* **8**, 7528-7536
396 (2017).
397 19. Cui, M., Lin, R. & Jia, G. Chemistry of Metallacyclobutadienes. *Chem. - Asian J.*

13, 895-912 (2018).

20. Rosenthal, U. Reactions of Group 4 Metallocene Bis(trimethylsilyl)acetylene Complexes with Nitriles and Isonitriles. *Angew. Chem., Int. Ed.* **57**, 14718-14735 (2018).

21. Schrock, R. R. Multiple Metal-Carbon Bonds for Catalytic Metathesis Reactions (Nobel Lecture). *Angew. Chem., Int. Ed.* **45**, 3748-3759 (2006).

22. Diver, S. T. & Giessert, A. J. Enyne Metathesis (Enyne Bond Reorganization). *Chem. Rev.* **104**, 1317-1382 (2004).

23. Fürstner, A. Alkyne Metathesis on the Rise. *Angew. Chem., Int. Ed.* **52**, 2794-2819 (2013).

24. Roland, C. D., Li, H., Abboud, K. A., Wagener, K. B. & Veige, A. S. Cyclic polymers from alkynes. *Nat. Chem.* **8**, 791-796 (2016).

25. Lv, Z. J., Chai, Z., Zhu, M., Wei, J. & Zhang, W. X. Selective Coupling of Lanthanide Metallacyclopropenes and Nitriles via Azametallacyclopentadiene and η^2-Pyrimidine Metallacycle. *J. Am. Chem. Soc.* **143**, 9151-9161 (2021).

26. Li, C., Dinoi, C., Coppel, Y. & Etienne, M. C-H Bond Activation of Methane by a Transient η^2-Cyclopropene/Metallabicyclobutane Complex of Niobium. *J. Am. Chem. Soc.* **137**, 12450-12453 (2015).

27. Hoffbauer, M. R. & Iluc, V. M. [2+2] Cycloadditions with an Iron Carbene: A Critical Step in Enyne Metathesis. *J. Am. Chem. Soc.* **143** (15), 5592-5597 (2021).

28. Lv, Z. J., Huang, Z., Shen, J., Zhang, W. X. & Xi, Z. Well-Defined Scandacyclopropenes: Synthesis, Structure, and Reactivity. *J. Am. Chem. Soc.***141**,

20547-20555 (2019).

29. Fang, B. *et al*. An Actinide Metallacyclopropene Complex: Synthesis, Structure, Reactivity, and Computational Studies. *J. Am. Chem. Soc.* **136**, 17249-17261 (2014).

30. Harrison, D. J. *et al*. Nickel Fluorocarbene Metathesis with Fluoroalkenes. *Angew. Chem., Int. Ed.* **57**, 5772-5776 (2018).

31. O'Connor, J. M. *et al*. Conversion of a Metallacyclobutene to Cobalt−Allene Complexes. *J. Am. Chem. Soc.* **120**, 1100-1101 (1998).

32. McGowan, K. P., O'Reilly, M. E., Ghiviriga, I., Abboud, K. A. & Veige, A. S. Compelling mechanistic data and identification of the active species in tungsten-catalyzed alkyne polymerizations: conversion of a trianionic pincer into a new *tetraanionic* pincer-type ligand. *Chem. Sci.* **4**, 1145-1155 (2013).

33. Kurogi, T., Pinter, B. & Mindiola, D. J. Methylidyne Transfer Reactions with Niobium. *Organometallics* **37**, 3385-3388 (2018).

34. Zhu, C. & Xia, H. Carbolong Chemistry: A Story of Carbon Chain Ligands and Transition Metals. *Acc. Chem. Res.* **51**, 1691-1700 (2018).

35. Zhu, C. *et al*. Stabilization of anti-aromatic and strained five-membered rings with a transition metal. *Nat. Chem.* **5**, 698-703 (2013).

36. Zhu, C. *et al*. Stabilizing Two Classical Antiaromatic Frameworks: Demonstration of Photoacoustic Imaging and the Photothermal Effect in Metalla-aromatics. *Angew. Chem., Int. Ed.* **54**, 6181-6185 (2015).

37. Torres-Alacan, J. *et al*. Photochemistry of a Puckered Ferracyclobutadiene in Liquid Solution Studied by Time-Resolved Fourier-Transform Infrared Spectroscopy. *Chem.*

- *Eur. J.* **21**, 17184-17190 (2015).

38. Zhuo, Q. *et al*. Constraint of a ruthenium-carbon triple bond to a five-membered ring. *Sci. Adv.* **4**, eaat0336 (2018).

39. Buil, M. L., Cardo, J. J., Esteruelas, M. A. & Onate, E. Square-Planar Alkylidyne–Osmium and Five-Coordinate Alkylidene–Osmium Complexes: Controlling the Transformation from Hydride-Alkylidyne to Alkylidene. *J. Am. Chem. Soc.* **138**, 9720-9728 (2016).

40. Batuecas, M. *et al*. Aromatic Osmacyclopropenefuran Bicycles and Their Relevance for the Metal-Mediated Hydration of Functionalized Allenes. *Angew. Chem., Int. Ed.* **55**, 13749-13753 (2016).

41. Clark, G. R., Lu, G.-L., Roper, W. R. & Wright, L. J. Stepwise Reactions of Acetylenes with Iridium Thiocarbonyl Complexes To Produce Isolable Iridacyclobutadienes and Conversion of These to either Cyclopentadienyliridium or Tethered Iridabenzene Complexes. *Organometallics* **26**, 2167-2177 (2007).

42. Schrock, R. R., Murdzek, J. S., Freudenberger, J. H., Churchill, M. R. & Ziller, J. W. Preparation of Molybdenum and Tungsten Neopentylidyne Complexes of the Type $M(CCMe_3)(O_2CR)_3$, Their Reactions with Acetylenes, and the X-ray Structure of the η^3-Cyclopropenyl Complex $W[C_3(CMe_3)Et_2](O_2CCH_3)_3$. *Organometallics* **5**, 25-33 (1986).

43. Weinstock, I. A., Schrock, R. R. & Davis, W. M. Rhenium(VII) Monoimido Alkylidyne Complexes. The Importance of Face Selectivity in the Metathesis of Acetylenes via Rhenacyclobutadiene Intermediates. *J. Am. Chem. Soc.* **113**, 135-144

(1991).

44. Zhu, C. *et al*. Planar Möbius aromatic pentalenes incorporating 16 and 18 valence electron osmiums. *Nat. Commun.* **5**, 3265 (2014).

45. Chen, Z., Wannere, C. S., Corminboeuf, C., Puchta, R. & Schleyer, P. Nucleus-Independent Chemical Shifts (NICS) as an Aromaticity Criterion. *Chem. Rev.* **105**, 3842-3888 (2005).

46. Geuenich, D., Hess, K., Kohler, F. & Herges, R. Anisotropy of the Induced Current Density (ACID), a General Method to Quantify and Visualize Electronic Delocalization. *Chem. Rev.* **105**, 3758-3772 (2005).

47. Wheeler, S. E., Houk, K. N., Schleyer, P. & Allen, W. D. A hierarchy of homodesmotic reactions for thermochemistry. *J. Am. Chem. Soc.* **131**, 2547-2560 (2009).

48. Oki, K., Takase, M., Mori, S. & Uno, H. Synthesis and Isolation of Antiaromatic Expanded Azacoronene via Intramolecular Vilsmeier-Type Reaction. *J. Am. Chem. Soc.* **141**, 16255-16259 (2019).

49. Ueta, K. *et al*. *meso*-Oxoisocorroles: Tunable Antiaromaticity by Metalation and Coordination of Lewis Acids as Well as Aromaticity Reversal in the Triplet Excited State. *J. Am. Chem. Soc.* **143**, 7958-7967 (2021).

Acknowledgments

This work was supported by the Natural Science Foundation of China (Nos. 22071206, 21931002 and 92156021), the Natural Science Foundation of Fujian Province of China (No. 2020J01025), the Shenzhen Science and Technology Innovation Committee (no. JCYJ20200109140812302), and the Guangdong Provincial Key Laboratory of Catalysis (no. 2020B121201002).

Author Contributions

H. X. and Y.-M. L. conceived the project. Y. L. performed the experiments. K. Z., Y. L., H. X. and Y.-M. L. analyzed and interpreted the experimental data. K. R. and Y. H. designed and performed the theoretical calculations. K. Z., Y. L. and Y.-M. L. prepared the manuscript. Y. L. and K. Z. prepared the Supplementary Information. All of the authors discussed the results and contributed to the preparation of the final manuscript.

Competing Interests

The authors declare no competing interests.

Additional Information

Supplementary Information (SI) is available for this paper at...

General information, preparation and characterization, crystallographic analysis, computational methods, NMR spectra and ESI-MS spectra (PDF)

Crystallographic data for **2a**, **3a**, **3b**, **3c**, **4A**, **5b**, and **6a** (CIF)

Reprints and permissions information are available at...

503 **Correspondence and requests for materials** should be addressed to H. X. and Y.-M.

504 L.

Supplementary Files

This is a list of supplementary files associated with this preprint. Click to download.

- SupplementaryInformation.pdf